



2014

# Intercellular propagated misfolding of wild-type Cu/Zn superoxide dismutase occurs via exosome-dependent and -independent mechanisms

Leslie I. Grad

*University of British Columbia*

Justin J. Yerbury

*University of Wollongong, jyerbury@uow.edu.au*

Bradley J. Turner

*University of Melbourne*

William C. Guest

*University of British Columbia*

Edward Pokrishevsky

*University of British Columbia*

*See next page for additional authors*

---

## Publication Details

Grad, L. I., Yerbury, J., Turner, B. J., Guest, W. C., Pokrishevsky, E., O'Neill, M. A., Yanai, A., Silverman, J. M., Zeineddine, R., Corcoran, L., Kumita, J. R., Luheshi, L. M., Yousefi, M., Coleman, B. M., Hill, A. F., Plotkin, S. S., Mackenzie, I. R. & Cashman, N. R. (2014). Intercellular propagated misfolding of wild-type Cu/Zn superoxide dismutase occurs via exosome-dependent and -independent mechanisms. *Proceedings of the National Academy of Sciences of USA*, 111 (9), 3620-3625.

---

# Intercellular propagated misfolding of wild-type Cu/Zn superoxide dismutase occurs via exosome-dependent and -independent mechanisms

## Abstract

Amyotrophic lateral sclerosis (ALS) is predominantly sporadic, but associated with heritable genetic mutations in 5-10% of cases, including those in Cu/Zn superoxide dismutase (SOD1). We previously showed that misfolding of SOD1 can be transmitted to endogenous human wild-type SOD1 (HuWtSOD1) in an intracellular compartment. Using NSC-34 motor neuron-like cells, we now demonstrate that misfolded mutant and HuWtSOD1 can traverse between cells via two nonexclusive mechanisms: protein aggregates released from dying cells and taken up by macropinocytosis, and exosomes secreted from living cells. Furthermore, once HuWtSOD1 propagation has been established, misfolding of HuWtSOD1 can be efficiently and repeatedly propagated between HEK293 cell cultures via conditioned media over multiple passages, and to cultured mouse primary spinal cord cells transgenically expressing HuWtSOD1, but not to cells derived from nontransgenic littermates. Conditioned media transmission of HuWtSOD1 misfolding in HEK293 cells is blocked by HuWtSOD1 siRNA knockdown, consistent with human SOD1 being a substrate for conversion, and attenuated by ultracentrifugation or incubation with SOD1 misfolding-specific antibodies, indicating a relatively massive transmission particle which possesses antibody-accessible SOD1. Finally, misfolded and protease-sensitive HuWtSOD1 comprises up to 4% of total SOD1 in spinal cords of patients with sporadic ALS (SALS). Propagation of HuWtSOD1 misfolding, and its subsequent cell-to-cell transmission, is thus a candidate process for the molecular pathogenesis of SALS, which may provide novel treatment and biomarker targets for this devastating disease.

## Disciplines

Medicine and Health Sciences

## Publication Details

Grad, L. I., Yerbury, J., Turner, B. J., Guest, W. C., Pokrishevsky, E., O'Neill, M. A., Yanai, A., Silverman, J. M., Zeineddine, R., Corcoran, L., Kumita, J. R., Luheshi, L. M., Yousefi, M., Coleman, B. M., Hill, A. F., Plotkin, S. S., Mackenzie, I. R. & Cashman, N. R. (2014). Intercellular propagated misfolding of wild-type Cu/Zn superoxide dismutase occurs via exosome-dependent and -independent mechanisms. *Proceedings of the National Academy of Sciences of USA*, 111 (9), 3620-3625.

## Authors

Leslie I. Grad, Justin J. Yerbury, Bradley J. Turner, William C. Guest, Edward Pokrishevsky, Megan A. O'Neill, Anat Yanai, Judith M. Silverman, Rafea Zeineddine, Lisa Corcoran, Janet Kumita, Leila Luheshi, Masoud Yousefi, Bradley M. Coleman, Andrew Hill, Steven S. Plotkin, Ian R. Mackenzie, and Neil R. Cashman

**Intercellular propagated misfolding of wild-type Cu-Zn superoxide dismutase occurs via exosome-dependent and independent mechanisms.**

**Running title:** Intercellular propagated misfolding of wild-type SOD1

**Classification:** Biological Sciences, Neuroscience

Leslie I. Grad<sup>a1</sup>, Justin J. Yerbury<sup>b1</sup>, Bradley J. Turner<sup>c1</sup>, William C. Guest<sup>a</sup>, Edward Pokrishevsky<sup>a</sup>, Megan A. O'Neill<sup>a</sup>, Anat Yanai<sup>a</sup>, Judith M. Silverman<sup>a</sup>, Rafea Zeineddine<sup>b</sup>, Lisa Corcoran<sup>b</sup>, Janet R. Kumita<sup>d</sup>, Leila Luheshi<sup>d</sup>, Masoud Yousefi<sup>a</sup>, Bradley M. Coleman<sup>e</sup>, Andrew F. Hill<sup>e</sup>, Steven S. Plotkin<sup>f</sup>, Ian R. Mackenzie<sup>g</sup> and Neil R. Cashman<sup>a2</sup>

<sup>1</sup>participated equally in the work

<sup>2</sup>To whom correspondence should be addressed

<sup>a</sup> Department of Medicine (Neurology) University of British Columbia and Vancouver Coastal Health Research Institute, Brain Research Centre, University of British Columbia, Vancouver, Canada V6T 2B5

<sup>b</sup> Illawarra Health and Medical Research Institute, University of Wollongong, Wollongong, Australia 2522

<sup>c</sup> Florey Institute of Neuroscience and Mental Health, University of Melbourne, Parkville, Australia 3010

<sup>d</sup> Department of Chemistry, University of Cambridge, Cambridge, UK, CB2 1EW

<sup>e</sup> Department of Biochemistry and Molecular Biology and Bio21 Molecular Science and Biotechnology Institute, University of Melbourne, Parkville, Australia 3010

<sup>f</sup> Department of Physics and Astronomy, University of British Columbia, Vancouver, Canada V6T 2B5

<sup>g</sup> Department of Pathology and Laboratory Medicine, University of British Columbia, Vancouver Canada V5Z 1M9

**Corresponding author:** Neil Cashman

Brain Research Centre, University of British Columbia

2211 Wesbrook Mall

Vancouver, Canada V6T 2B5

(604) 822-2135

[neil.cashman@vch.ca](mailto:neil.cashman@vch.ca)

**Key words:** amyotrophic lateral sclerosis, protein misfolding, superoxide dismutase, exosomes, intercellular transmission

**Significance Statement:** Amyotrophic lateral sclerosis (ALS), an incurable motor neuron disease, is associated with mutation and misfolding of the Cu/Zn superoxide dismutase (SOD1) protein. Prior studies found that mutant misfolded SOD1 can convert wild-type SOD1 to a misfolded form inside living cells in a prion-like fashion. We now report that misfolded wild-type SOD1 can be transmitted from cell to cell, and that propagated protein misfolding can be perpetuated. Misfolded SOD1 transmission between cells can be mediated through release and uptake of protein aggregates, or via small membrane-bounded transport vesicles, called exosomes. These mechanisms may help explain why sporadic ALS, without genetic mutation, can spread systematically from region to region in a progressive manner.

## **ABSTRACT**

Amyotrophic lateral sclerosis (ALS) is predominantly sporadic, but associated with heritable genetic mutations in 5-10% of cases, including those in Cu/Zn superoxide dismutase (SOD1). We previously showed that misfolding of SOD1 can be transmitted to endogenous human wild-type SOD1 (HuWtSOD1) in an intracellular compartment. Using NSC34 motor neuron-like cells, we now demonstrate that misfolded mutant and HuWtSOD1 can traverse between cells via two non-exclusive mechanisms: protein aggregates released from dying cells and taken up by macropinocytosis, and extracellular vesicles (exosomes) secreted from living cells. Furthermore, once HuWtSOD1 propagation has been established, misfolding of HuWtSOD1 can be efficiently and repeatedly propagated between HEK293 cell cultures via conditioned media over multiple passages, and to cultured mouse primary spinal cord cells transgenically expressing HuWtSOD1, but not to cells derived from non-transgenic littermates. Conditioned media transmission of HuWtSOD1 misfolding in HEK293 cells is blocked by HuWtSOD1 siRNA knockdown, consistent with human SOD1 being a substrate for conversion, and attenuated by ultracentrifugation or incubation with SOD1 misfolding-specific antibodies, indicating a relatively massive “transmission particle” which possesses antibody-accessible SOD1. Finally, misfolded and protease sensitive HuWtSOD1 comprises up to 4% of total SOD1 in sporadic ALS patient spinal cord. Propagation of HuWtSOD1 misfolding, and its subsequent cell-to-cell transmission, is thus a candidate process for the molecular pathogenesis of sporadic ALS, which may provide novel treatment and biomarker targets for this devastating disease.

\body

Amyotrophic lateral sclerosis (ALS) is a fatal neuromuscular condition that afflicts as many as 1 out of 350 males and 420 females over 18 (1). In ALS, degeneration of upper and lower motor neurons causes progressive muscle paralysis and spasticity, affecting mobility, speech, swallowing and respiration (2). Half of affected individuals die within 3 years, and less than 20% survive for more than 5 years (3). 90-95% of cases are sporadic (SALS) in which some apparently facilitating gene mutations, such as ataxin-2 repeat expansions (4), have been identified. The remaining 5-10% of cases are familial (FALS) and are predominantly associated with Mendelian-inherited mutations in Cu/Zn superoxide dismutase (SOD1), TAR-DNA binding protein 43 (TDP-43), fused in sarcoma/ translocated in liposarcoma (FUS/TLS), C9ORF72, and other genes (reviewed in (3)).

Despite the profusion of functionally diverse genes implicated in FALS and SALS, clinical and pathological similarities between all forms of ALS suggest the existence of a common pathogenic pathway that could be united by a single gene/protein (5). One of the mechanisms by which a mutant or wild-type (Wt) protein can dominate pathogenesis of phenotypically diverse diseases is by propagated protein misfolding, such as that underpinning the prion diseases, which has been increasingly implicated in other neurodegenerative and systemic disorders (6, 7). A role for propagated protein misfolding in ALS is supported by the prion-like spatiotemporal progression of disease through the neuroaxis (8, 9). However, given the disparity in protein inclusion pathology between subtypes of ALS, a single unifying prion-like protein that could explain such a progression remains obscure.

While it is generally accepted SOD1 is not found in large perikaryal cytoplasmic inclusions outside of SOD1 FALS cases, misfolded SOD1 has been increasingly identified in SALS and non-SOD1 FALS (5, 10, 11). Indeed, we have reported that misfolded HuWtSOD1 can be detected by spinal cord immunohistochemistry in FALS secondary to FUS mutation, and in SALS patients with cytosolic TDP-43 accumulation (11). Moreover, in cell models, over-expression of WtTDP-43, or expression of mutant FUS or TDP-43, is associated with HuWtSOD1 misfolding (11). Collectively, these data are consistent with SOD1 being a “molecular common denominator” for all types of ALS. Furthermore, prion-like activity has been described for the cell-to-cell transmission of misfolding of mutant SOD1 (12), and we have reported that mutant SOD1 can confer its misfold on HuWtSOD1 (13). However, mutant SOD1 cannot explain propagation in SALS.

In order to test if HuWtSOD1 participates in cell-to-cell transmission of protein misfolding, we make use of previously developed mouse monoclonal antibody probes for misfolded/oxidized SOD1, recognizing either full-length human mutant or wild-type SOD1 (HuWtSOD1), generated against regions that are antibody-inaccessible in natively folded SOD1 (13-15). Misfolded SOD1 mAbs employed in this work are 10E11C11 and 3H1, directed against an unstructured electrostatic loop (disease-specific epitope-2; DSE2), and 10C12, directed against a C-terminal dimer interface peptide in which the cysteine at position 146 is substituted by a cysteic acid residue to mimic oxidation of this residue (DSE1a; (13)). The use of such antibody probes have enabled us to unambiguously determine the role of misfolded mutant G127X in the induced misfolding of HuWtSOD1, which upon misfolding acquires a marked increase in sensitivity to protease digestion, consistent with global loosening of structure (13). The finding that

misfolded endogenous HuWtSOD1 was observed long after transfected G127X-SOD1 was degraded suggested that HuWtSOD1, once misfolded, is capable of triggering an *intracellular* propagated misfolding reaction (13). We now report for the first time that misfolded HuWtSOD1 can transit cell-to-cell both via exosomes, and release of protein aggregates and subsequent uptake in neuronal cells. In addition, misfolded HuWtSOD1 can sustain *intercellular* propagated misfolding *in vitro* and is detectable in the spinal cord of all ALS patients tested, regardless of the genetic etiology of the disease. Collectively, these data indicate that HuWtSOD1 is competent to participate in propagated misfolding, suggesting a common pathogenic mechanism linking FALS and SALS.

## Results

### Cellular import and export of the SOD1 transmission particle

Previous work would suggest that the release of misfolded proteins is likely to occur either through exocytosis or cell rupture due to death (16) while uptake is thought to be non-specific and mediated by fluid phase endocytosis (12). Mutant and HuWtSOD1 have been shown to be exported from NSC-34 cells via small vesicles known as exosomes (17), and a separate study shows that protein-only aggregates of mutant SOD1 are efficiently imported into mouse N2a cells by a macropinocytosis-dependent process (12). To more fully characterize possible intercellular transmission pathways of SOD1 misfolding we employed the murine motor neuron-like NSC-34 cell line (18). NSC-34 cells were transfected with HuWtSOD1-GFP or mutant SOD1-GFP variants; significant cell death was observed 72 hours post-transfection that was not prominent in transient GFP-alone transfection or in SOD1-GFP stably transfected models (**Fig. 1A**). SOD1-GFP aggregates are observed in transiently transfected NSC-34 cells, but not in stably-transfected ones (**Fig. S1**). Taken together, these data demonstrate the neuron-like susceptibility of NSC-34 cells to neurotoxic species of SOD1 (19). At this time-point SOD1-GFP positive particles, both HuWt and mutants, could be transferred to naïve cells via conditioned medium transfer and uptake of these particles could be detected in naïve NSC-34 cells (**Fig. 1B**). This uptake appeared specific as GFP by itself was not detected inside naïve cells. Given that the transmitted particle may be a complex mix of both released exosomes and protein aggregates, the conditioned medium was analyzed by immunoblot to determine if SOD1 aggregates were released from the dying NSC-34 cells, revealing SDS-resistant oligomers released by cells transfected with SOD1-GFP variants, including HuWtSOD1 (**Fig. 1C**). Filter trap analysis confirmed aggregates larger than the 0.2  $\mu\text{m}$  pore size in conditioned medium supernatants from dying NSC-34 cells transfected with all SOD1-GFP variants (**Fig. 1D, E**), including HuWtSOD1-GFP. To determine if non-vesicular protein-only SOD1 aggregates can be taken up by naïve NSC-34 cells, recombinant HuWtSOD1 protein was firstly pre-aggregated by a seeding event initiated by mutant misfolded G93A SOD1 (**Fig. S2A-D**). Flow cytometry with confocal microscopy demonstrated that aggregated HuWtSOD1 is incorporated by NSC-34 cells (**Fig. 1F, S2E**), and that this process is mediated by macropinocytosis, as the specific inhibitor 5-(N-ethyl-N-isopropyl)-amiloride (EIPA), but not the clathrin-coated pit inhibitor chlorpromazine hydrochloride (CPZ), the caveolin-dependent inhibitor genestein, or lipid raft pathway inhibitor methyl- $\beta$ -cyclodextrin (M $\beta$ CD), suppressed aggregated HuWtSOD1 uptake (**Fig. S2F**). Furthermore, uptake is SOD1-specific and aggregated forms are taken up as efficiently as non-aggregated forms, while the control protein, GST, was not taken up at all. (**Fig. S2G**).

Although our transiently transfected model indicates that large aggregates of misfolded SOD1 from dead or dying cells can be efficiently taken up by neighbouring cells, we and others have found that exosomal-mediated transport is relevant for misfolded protein transmission in living cells (17, 20), for which we utilized stably transfected NSC-34 cells that show little cell death (**Fig. 1A**). Exosomal fractions were isolated from these cells as previously described (17), with an additional high-speed (100,000 x *g*) centrifugation step included following washing to ensure microvesicles are sufficiently depleted of non-specific material. Visualization of ultracentrifuged pellets from conditioned medium collected from cultures of stably transfected NSC-34 cells revealed microvesicles that were membrane-bounded, consistent with exosomes in morphology and size of ~100 nm (**Fig. 1G**). Exosome pellets showed enrichment of TSG101 and flotillin 1 compared to cell lysates confirming their endosomal origin (**Fig. S3A**) and the presence of PrP on the membrane surface by immunoelectron microscopy, another marker of exosomes (**Fig. S3B**). Immunoelectron microscopy with the 3H1 SOD1 misfolding-specific antibody revealed that ~80-90% of grains were associated with the exterior of exosomes secreted by cells stably expressing mutant or HuWtSOD1 (**Fig. 1H**), with only a small minority labeling apparent protein aggregates not in proximity to exosomes (**Fig. 1I**). Immunoelectron microscopy of HuWtSOD1-GFP exosomes also revealed robust immunoreactivity for the C-terminal misfolded/oxidized SOD1 mAb 10C12 (**Fig. S3C**), but not the C4F6 mAb directed at more N-terminal residues 80-118 (5) (**Fig. S3D**), implying that the C-terminal third of SOD1 is preferentially exposed on the outside surface of exosomes. The configuration of misfolded SOD1 associated with the surface of exosomes was not an artifact of the GFP tag as 3H1 also labeled non-tagged mutant or HuWtSOD1 exosomes from stably transfected NSC-34 cells (**Fig. S3E**). Flow cytometry and confocal microscopy of naïve NSC-34 cells exposed to exosomes secreted from cells stably expressing HuWtSOD1-GFP revealed that exosome uptake was relatively efficient (**Fig. 1J, S3F**).

### **HuWtSOD1 misfolding can be transmitted intercellularly**

Aggregation of soluble intracellular mutant SOD1 has been observed upon media exposure to the same mutants in an aggregated state (12), and we have shown that mutant SOD1 induces the misfolding of HuWtSOD1 when transfected in human, but not mouse, cell lines (13). Furthermore, we show that misfolded SOD1, both wild-type and mutant, may be exported from cells either associated with exosomes or as protein-only aggregates. Thus, we investigated whether cells containing mutant-induced misfolded HuWtSOD1 acquire the capacity to transmit misfolded SOD1 from cell-to-cell, and whether such misfolded protein could act as propagating seeds in untransfected naïve cell cultures (schematically shown in **Fig. S4A**). We selected the mesenchymal HEK293 cell line for their expression of substrate HuWtSOD1, their resistance to the toxicity of misfolded SOD1, and their efficiency of transfection (13). DSE-immunoprecipitable misfolded HuWtSOD1 was detected in lysates of HEK293 cells incubated overnight with conditioned media from HEK293 cells transiently transfected with G127X mutant SOD1, but not from lysates in which cells were incubated with media from a control empty vector transfection (**Fig. 2A, S4B**), reminiscent of the transfer observed in NSC-34 cells (**Fig. 1B**). Incubation of naïve HEK293 cells with media from cultures transiently transfected with green fluorescent protein (GFP) did not induce SOD1 misfolding (**Fig S4C**), demonstrating that the misfolding of HuWtSOD1 in human recipient cells is specifically induced by a conditioned medium factor from SOD1-transfected HEK293 cells.



Misfolded SOD1 content in recipient culture lysates was unaffected by DNase digestion of conditioned media (**Fig. S4D**), ruling out a contribution of residual transfection plasmid. Consistent with prion-like propagated misfolding of HuWtSOD1, SOD1 misfolding could be serially passaged from culture to culture via sequential media incubation (shown schematically in **Fig. S4A**, and experimentally to at least five passages in **Fig. 2A**). It is notable that from the first passage onward, the DSE-immunoprecipitable misfolded SOD1 in lysates migrated as HuWtSOD1, despite being incubated with supernatants of cells transfected with the faster-migrating SOD1 mutants G127X and G85R, suggesting that misfolded HuWtSOD1 was competent to transmit its acquired conformation between cell cultures (**Fig. 2A, S4E**). Forced over-expression of HuWtSOD1 in the initial transfection HEK293 cultures (associated with SOD1 misfolding (13, 21)) also resulted in efficient transmission of SOD1 misfolding via media, which did not diminish with multiple serial passage (**Fig. 2A**), indicating that HuWtSOD1 was indeed fully competent to support misfolding propagation in a self-sustaining reaction. To confirm the capacity of HuWtSOD1 to mediate prion-like propagated misfolding transmission between cells, we depleted endogenous HuWtSOD1 expression in HEK293 cells with siRNA oligonucleotides prior to exposure to conditioned media. SOD1-DSE immunoprecipitations of lysates from HuWtSOD1-depleted cells revealed drastically reduced misfolded HuWtSOD1 compared to control incubations (**Fig. 2B, S5A**), arguing against the observed misfolded HuWtSOD1 resulting solely from SOD1 uptake from conditioned media, and consistent with recipient cell endogenous HuWtSOD1 being an authentic substrate for propagated protein misfolding. We also observed transmission of propagated SOD1 misfolding to primary neural cultures derived from embryonic mouse spinal cord expressing HuWtSOD1 when exogenously applied mutant misfolded SOD1 in conditioned medium is present (**Fig. 2C; Fig. S5B**), confirming that the process occurs in a physiologically relevant system.

### **Intercellular transmission is mediated by particles displaying misfolded SOD1**

The majority of DSE-immunoprecipitable SOD1 was detectable in the ultracentrifuged pellets of conditioned media from mutant SOD1 transfected cells (**Fig. 3A**). Naïve cells were incubated with re-suspended pellet or supernatant fractions of ultracentrifuged (100,000 *g* X 1hr) conditioned media obtained from cells transfected with mutant or wild-type constructs of SOD1. Lysates from incubated cells revealed that ~80% of the HuWtSOD1 misfolding activity was present in the pellet fraction (**Fig. S6A**), consistent with a relatively massive “transmission particle” composed of protein-only aggregates, associated with exosomes, or both. Surface plasmon resonance analysis of pellet fractions derived from conditioned media revealed 3H1-immunoreactive misfolded SOD1, even in G127X-transfected supernatants (**Fig. 3B**), signifying the extracellular presence of misfolded full-length SOD1, and consistent with exposed misfolded HuWtSOD1 being a component of the transmission particle. In the special case of G127X, for which we have generated a mutant-specific rabbit polyclonal antibody (13), we detected limited G127X protein in G127X-transfected HEK293 supernatants (**Fig. S6B**), suggesting that on first transmission mutant SOD1 may participate in the cell-to-cell propagation of SOD1 misfolding. However, sequential dilution of mutant SOD1 in subsequent passages would militate against mutant SOD1 being an essential component of the intercellular transmission particle, and indeed in serial passages kindled by transfection by HuWtSOD1 (**Fig. 2A**), mutant SOD1 formally cannot participate. Exposure of misfolded SOD1 epitopes in the transmission particle suggests that cell-to-cell

transmission might be neutralized by antibodies directed against misfolded or native HuWtSOD1. Following the blocking protocol schematically shown in **Fig. S4A**, the HuWtSOD1 converting activity of conditioned media from G127X- or G85R-transfected HEK293 cells was abolished by pre-incubation with SOD1-specific polyclonal rabbit IgG, but not control rabbit IgG (**Fig. 4A, B**). Furthermore, HuWtSOD1 conversion in naïve HEK293 cells exposed to the conditioned medium of HEK293 cells transfected with G127X, G85R or HuWtSOD1 was attenuated by DSE mAbs 3H1 and 10C12 expected to react with full-length misfolded/oxidized isoforms of SOD1 (**Fig. 4A-C**), in keeping with misfolded HuWtSOD1 being an accessible and essential component of the cell-to-cell transmission particle.

### **Aggregates of misfolded HuWtSOD1 are present in ALS patient spinal cords**

Using the DSE mAbs, we have previously demonstrated the presence of misfolded/oxidized SOD1 by immunohistochemistry (IHC) in SOD1- and FUS-FALS, and in SALS with cytoplasmic TDP43 accumulation (11). To confirm the presence of misfolded HuWtSOD1 in ALS pathology *in vivo*, we examined a larger series of IHC of post-mortem human spinal cord sections from control, mutant-SOD1 FALS, non-SOD1 FALS (including two cases due to expansion mutations in the *C9ORF72* gene (22, 23)), and SALS patients (including one case of *C9ORF72* expansion without family history of ALS; **Table S1**). In all cases of ALS examined, regardless of SOD1 sequence, we detected immunoreactivity with the DSE mAbs within motor neurons (N=28; **Fig. 5A-F**). Similar types of structures were stained by the DSE mAbs in all ALS tissue samples, although there were appreciable differences in distribution (**Table S2**), with mutant SOD1-FALS showing numerous neuronal cytoplasmic inclusions that were rare in SALS and *C9ORF72*-FALS, in addition to axonal and tract immunoreactivity observed in all types of ALS. However, IHC may not accurately represent the total amount of misfolded SOD1, likely missing soluble monomers or oligomers immunoreactive with the DSE mAbs. We thus performed quantitative immunoprecipitation (IP) from unfixed spinal cord homogenates with DSE mAbs, normalized to total SOD1 immunoprecipitated with a pan-SOD1 polyclonal antibody (pAb). IP experiments were conducted using homogenates of post-mortem cervical or thoracic spinal cord from patients with mutant-SOD1 FALS and non-SOD1 SALS (including one case with *C9ORF72* expansion without family history; **Fig. 5G**; 'SALS 2, C'), as well as controls (**Fig. 5G**; **Table S3**). Spinal cords from Alzheimer's disease (AD) patients (N=3) were included as a neurological disease control, along with age- and sex-matched control spinal cord samples from normal subjects (N=4). Misfolded/oxidized SOD1 was detected in unexpectedly high concentration of ~4% in SOD1-FALS, and SALS, including one case of *C9ORF72* mutation without family history of ALS (**Fig. 5G, S7A**). The amount of SOD1 immunoprecipitated by the DSE mAbs was not significantly above background in either AD or other control samples.

Similar to our previous demonstration of acquisition of protease sensitivity by induced misfolding *in vitro* (13), we found that that DSE-immunoreactive SOD1 species *in vivo* acquired profound sensitivity to protease digestion when we subjected FALS and SALS spinal cord homogenates to proteinase K (PK) digestion at a concentration of 200 µg/ml (**Fig. 5G**). PK treatment significantly decreased DSE-immunoprecipitable SOD1 by 85-90% for FALS and SALS for both DSE antibodies (**Fig. S7A**). Titrated PK-digestion of control homogenates reveals that native HuWtSOD1 is highly resistant to PK digestion, even at concentrations 100-fold higher (**Fig. S7B**). Detergent-insoluble oligomers of similar intensity are

observed in spinal cord homogenate from both FALS and SALS patients, in contrast to control and AD samples (Fig. S7C, D); similar observations have been made in SOD1 mouse models of ALS (24).

## Discussion

Increasing evidence supports the notion that progression of pathology in neurodegenerative diseases such as Alzheimer's disease, Parkinson's disease, tauopathies and Huntington's disease is a result of propagation of misfolded or aggregated proteins (6, 7, 16). The capability of a pathogenic protein conformation to self-propagate is the central tenant of the prion hypothesis, with a necessary requirement of sporadic prion diseases being that the process of conformational conversion must be capable of being mediated by the un-mutated, wild-type PrP. Mutant SOD1 has been shown to confer its misfolded aggregated phenotype on soluble mutant SOD1 (12). Until this report, unambiguous evidence of the competence of HuWtSOD1 in propagated protein misfolding has been lacking. We and others detect SOD1 misfolding in SALS and non-SOD1 FALS, in addition to SOD1 FALS (5, 10) and here we present data that indicates that misfolded and protease-sensitive HuWtSOD1 is present in the spinal cord of SALS patients, representing ~ 4% of total SOD1. Although we cannot rule out the possibility that SOD1 misfolding is a consequence of SALS pathology, taken together, these data suggest propagated misfolding of SOD1 is a strong candidate for a downstream "final common pathway" for all types of ALS, including its sporadic form.

We report here that HuWtSOD1 efficiently propagates from cell-to-cell in a HuWtSOD1 expression-dependent process by two non-exclusive mechanisms: release of protein-only aggregates and cell derived vesicles identified as exosomes. It might be expected that aggregates of "naked" misfolded SOD1 might be exported from cells as they die. Fibrils of SOD1 have already been shown to be a competent seed for further SOD1 aggregation *in vitro* (25), and when exogenously applied can be efficiently taken up into living cells (26). In addition, aggregates of mutant SOD1 have been observed to be taken up into neuron-like cells via macropinocytosis (12). In both cases the multimeric structures of SOD1 provide competent seeds for aggregation of soluble mutant SOD1, suggesting SOD1 aggregates to be an efficient means of misfolding propagation between cells. Our data also indicates that macropinocytosis is implicated in the uptake of aggregated HuWtSOD1, also known to be involved in the propagation of mutant SOD1 aggregation (12). Although we have not identified the receptors involved in this process our previous work on microglia would suggest a large receptor complex involving scavenger or other pattern recognition receptors and signaling receptors may be participating (27). Heparin sulphate proteoglycans have been shown to be involved in aggregate uptake of tau, alpha-synuclein and prion protein (28, 29), and it is interesting to speculate that this family of receptors could be involved here. However, before cell death ensues in ALS or other neurodegenerative diseases, pathology can spread from cell-to-cell and region to region (8), suggesting another mechanism that may be more relevant to early stages of the disease. We propose that export and uptake may be mediated by a pathological hijacking of exosome biology, which has been theorized to participate in prion propagation, and other proteopathic neurodegenerative diseases such as Alzheimer's and Parkinson's disease (reviewed in (30)). Exosomes can interact with neighbouring cells by various mechanisms, including direct fusion with recipient plasma membrane, endocytosis and fusion with endosomal membrane, receptor-mediated endocytosis and phagocytosis (31). Most recently, exosome uptake by

macropinocytosis was found (32) which could lead to release of exosomal SOD1 and propagation-competent seeds delivered into the cytosol of a neighboring cell.

Importantly, the cell-to-cell transmission of SOD1 misfolding can be neutralized with antibodies directed against misfolded SOD1, which is consistent with either naked aggregate transfer, or transfer via the antibody-accessible surface of exosomes. Indeed, prion or amyloid- $\beta$  containing exosomes are not limited by the interior release of misfolded or aggregated protein or peptides. Most significantly, the inhibition of propagated misfolding of SOD1 by misfolding-specific antibodies *in vitro* suggests a novel immunotherapeutic approach to neutralizing the spread of disease in ALS patients. We note that *in vitro* neutralization apparently correlates with exosome exposure of misfolding-specific epitopes 3H1 and 10C12; however, an antibody directed against an epitope not exposed on the surface of exosomes, C4F6, is not effective in treatment of mouse models of ALS (33). Thus, restrictions may exist on exposure of the cognate epitopes *in vivo*, due to aggregation sequestration or topological constraints of misfolded SOD1 on exosome membranes. It may prove important to understand the immunological anatomy of misfolded SOD1 to generate effective immunotherapies for ALS.

## Materials and Methods

**Electron microscopy.** Exosomes were fixed in 2% PFA in PBS for 10 min and applied to glow-discharged 200 mesh Cu grids coated with formvar-carbon film (ProSciTech, Kirwin, Australia) and absorbed for 20 min. Grids were washed twice (PBS, 3 min) and blocked with 5% (w/v) BSA in PBS for 15 min followed by staining with 3H1 (1:200), 10C12 (1:200) or C4F6 (1:50) in PBS, 0.1% BSA for 30 min. Grids were washed 6 times and incubated with Aurion Protein-G gold 10nm (ProSciTech) in PBS for 90 min. Grids were washed, post-fixed with 2% glutaraldehyde in PBS for 10 min, washed again, contrasted with 1.5% uranyl acetate and viewed with a 300kV Tecnai G2 F30 electron microscope (FEI). Exosomal and proximate free 3H1-positive grains were counted from 5 micrographs per cell line and expressed as % of total 3H1-positive grains.

**Release of SOD1 aggregates.** NSC-34 cells were transfected with HuWtSOD1-GFP, G127X SOD1-GFP, G93A SOD1-GFP or A4V SOD1-GFP. After 72 hours the conditioned media was collected as above and 50 µg of total protein was then analyzed by filter trap assay or western blot. The filter trap assay was performed as previously reported (34). Any trapped SOD1-GFP material was measured using an anti-GFP antibody. Conditioned media was centrifuged at 13,000 x *g* on a benchtop microfuge for 30 min and pellets resuspended in PBS. Pelleted material was then added on to naïve NSC-34 cells and incubated for 60 minutes at 37°C. The cells were then fixed and permeabilized and internalized SOD1-GFP was measured using flow cytometry (BD LSR II; BD Biosciences, Franklin Lakes, NJ).

**Immunoprecipitation.** Immunoprecipitation of cell lysate and preparation of antibody-coupled beads were performed as previously described (13). Following IP incubation, beads were washed three times with 150 µl PBS with brief vortexing in between washes and boiled in SDS sample buffer. Samples were loaded onto 15% acrylamide Tris-glycine gels and separated by SDS-PAGE, followed by immunoblotting. Immunoblotting, detection and quantification were performed as previously described (13).

## **Acknowledgements**

NRC is the Canada Research Chair in Neurodegeneration and Protein Misfolding Diseases at the University of British Columbia, and is supported by donations from the Webster Foundation, the Allen T. Lambert Neural Research Fund and the Temerty Family Foundation, and also by grants from PrioNet Canada, the Canadian Institutes of Health Research (CIHR), and Biogen-Idec Corp. JJY is supported by the MND Research Institute of Australia and by NHMRC project grant 1003032. BJT is supported by NHMRC Project Grant 1008910 and MND Research Institute of Australia Mick Rodger Benalla MND Research Grant. AFH is an Australian Research Council Future Fellow (FT3) and supported by an NHMRC Program Grant 628946. Proprietary antibodies against misfolded SOD1 and additional funding were provided by Amorfix Life Sciences. NRC declares that he is Founder, Chief Scientific Officer and Chairman of Amorfix Life Sciences.

## References

1. Armon C (2007) Sports and trauma in amyotrophic lateral sclerosis revisited. *J Neurol Sci* 262(1-2):45-53.
2. Hardiman O, van den Berg LH, & Kiernan MC (2011) Clinical diagnosis and management of amyotrophic lateral sclerosis. *Nat Rev Neurol* 7(11):639-649.
3. Robberecht W & Philips T (2013) The changing scene of amyotrophic lateral sclerosis. *Nat Rev Neurosci* 14(4):248-264.
4. Elden AC, et al. (2010) Ataxin-2 intermediate-length polyglutamine expansions are associated with increased risk for ALS. *Nature* 466(7310):1069-1075.
5. Bosco DA, et al. (2010) Wild-type and mutant SOD1 share an aberrant conformation and a common pathogenic pathway in ALS. *Nat Neurosci* 13(11):1396-1403.
6. Guest WC, et al. (2011) Generalization of the prion hypothesis to other neurodegenerative diseases: an imperfect fit. *J Toxicol Environ Health A* 74(22-24):1433-1459.
7. Prusiner SB (2012) Cell biology. A unifying role for prions in neurodegenerative diseases. *Science* 336(6088):1511-1513.
8. Ravits JM & La Spada AR (2009) ALS motor phenotype heterogeneity, focality, and spread: deconstructing motor neuron degeneration. *Neurology* 73(10):805-811.
9. Polymenidou M & Cleveland DW (2011) The seeds of neurodegeneration: prion-like spreading in ALS. *Cell* 147(3):498-508.
10. Forsberg K, et al. (2010) Novel antibodies reveal inclusions containing non-native SOD1 in sporadic ALS patients. *PLoS ONE* 5(7):e11552.
11. Pokrishevsky E, et al. (2012) Aberrant localization of FUS and TDP43 is associated with misfolding of SOD1 in amyotrophic lateral sclerosis. *PLoS ONE* 7(4):e35050.
12. Munch C, O'Brien J, & Bertolotti A (2011) Prion-like propagation of mutant superoxide dismutase-1 misfolding in neuronal cells. *Proc Natl Acad Sci U S A* 108(9):3548-3553.
13. Grad LI, et al. (2011) Intermolecular transmission of superoxide dismutase 1 misfolding in living cells. *Proc Natl Acad Sci U S A* 108(39):16398-16403.
14. Rakhit R, et al. (2007) An immunological epitope selective for pathological monomer-misfolded SOD1 in ALS. *Nat Med* 13(6):754-759.
15. Vande Velde C, Miller TM, Cashman NR, & Cleveland DW (2008) Selective association of misfolded ALS-linked mutant SOD1 with the cytoplasmic face of mitochondria. *Proc Natl Acad Sci U S A* 105(10):4022-4027.
16. Brundin P, Melki R, & Kopito R (2010) Prion-like transmission of protein aggregates in neurodegenerative diseases. *Nat Rev Mol Cell Biol* 11(4):301-307.
17. Gomes C, Keller S, Altevogt P, & Costa J (2007) Evidence for secretion of Cu,Zn superoxide dismutase via exosomes from a cell model of amyotrophic lateral sclerosis. *Neurosci Lett* 428(1):43-46.
18. Cashman NR, et al. (1992) Neuroblastoma x spinal cord (NSC) hybrid cell lines resemble developing motor neurons. *Dev Dyn* 194(3):209-221.
19. Gomes C, et al. (2008) Establishment of a cell model of ALS disease: Golgi apparatus disruption occurs independently from apoptosis. *Biotechnol Lett* 30(4):603-610.
20. Bellingham SA, Guo BB, Coleman BM, & Hill AF (2012) Exosomes: vehicles for the transfer of toxic proteins associated with neurodegenerative diseases? *Front Physiol* 3:124.
21. Graffmo KS, et al. (2013) Expression of wild-type human superoxide dismutase-1 in mice causes amyotrophic lateral sclerosis. *Hum Mol Genet* 22(1):51-60.
22. DeJesus-Hernandez M, et al. (2011) Expanded GGGGCC hexanucleotide repeat in noncoding region of C9ORF72 causes chromosome 9p-linked FTD and ALS. *Neuron* 72(2):245-256.

23. Renton AE, *et al.* (2011) A hexanucleotide repeat expansion in C9ORF72 is the cause of chromosome 9p21-linked ALS-FTD. *Neuron* 72(2):257-268.
24. Furukawa Y, Fu R, Deng HX, Siddique T, & O'Halloran TV (2006) Disulfide cross-linked protein represents a significant fraction of ALS-associated Cu, Zn-superoxide dismutase aggregates in spinal cords of model mice. *Proc Natl Acad Sci U S A* 103(18):7148-7153.
25. Chia R, *et al.* (2010) Superoxide dismutase 1 and tgSOD1 mouse spinal cord seed fibrils, suggesting a propagative cell death mechanism in amyotrophic lateral sclerosis. *PLoS ONE* 5(5):e10627.
26. Furukawa Y, Kaneko K, Watanabe S, Yamanaka K, & Nukina N (2013) Intracellular seeded aggregation of mutant Cu,Zn-superoxide dismutase associated with amyotrophic lateral sclerosis. *FEBS Lett* 587(16):2500-2505.
27. Roberts K, *et al.* (2013) Extracellular aggregated Cu/Zn superoxide dismutase activates microglia to give a cytotoxic phenotype. *Glia* 61(3):409-419.
28. Horonchik L, *et al.* (2005) Heparan sulfate is a cellular receptor for purified infectious prions. *J Biol Chem* 280(17):17062-17067.
29. Holmes BB, *et al.* (2013) Heparan sulfate proteoglycans mediate internalization and propagation of specific proteopathic seeds. *Proc Natl Acad Sci U S A* 110(33):E3138-3147.
30. Vella LJ, Sharples RA, Nisbet RM, Cappai R, & Hill AF (2008) The role of exosomes in the processing of proteins associated with neurodegenerative diseases. *Eur Biophys J* 37(3):323-332.
31. Thery C, Ostrowski M, & Segura E (2009) Membrane vesicles as conveyors of immune responses. *Nat Rev Immunol* 9(8):581-593.
32. Fitzner D, *et al.* (2011) Selective transfer of exosomes from oligodendrocytes to microglia by macropinocytosis. *J Cell Sci* 124(Pt 3):447-458.
33. Gros-Louis F, Soucy G, Lariviere R, & Julien JP (2010) Intracerebroventricular infusion of monoclonal antibody or its derived Fab fragment against misfolded forms of SOD1 mutant delays mortality in a mouse model of ALS. *J Neurochem* 113(5):1188-1199.
34. Matsumoto G, Stojanovic A, Holmberg CI, Kim S, & Morimoto RI (2005) Structural properties and neuronal toxicity of amyotrophic lateral sclerosis-associated Cu/Zn superoxide dismutase 1 aggregates. *J Cell Biol* 171(1):75-85.



## Figure Legends

### Figure 1. Aggregated SOD1 is released from dead or dying cells and/or actively released as part of exosomes.

(A) Cell death of GFP-positive cells after 72 hours post-transfection was examined by flow cytometry. Cells stained with PI were scored as dead and these cells expressed as a proportion of total GFP positive cells. The results are means and standard error of three independent experiments. (B) Uptake of pelletable SOD1-GFP by naïve NSC-34 cells following incubation with conditioned media was measured by flow cytometry. The data shown is calculated from triplicate experiments. Error bars represent SEM and \* indicates statistical significance ( $P < 0.05$ ) compared to medium from non-transfected (NT) cells, as determined by unpaired *t*-test. (C) Detection of oligomeric SOD1 released into media 72 hours post-transfection. White arrow indicates SOD1-GFP monomer while black arrow indicates SOD1-GFP dimer. Area indicated by \* represents SDS-resistant oligomeric SOD1 species. Immunoblot probed with GFP polyclonal antibody. (D) Filter-trap assay and anti-GFP immunoblot to detect SOD1-GFP aggregates in conditioned media. The filter trap was performed in triplicate and is quantified in (E). Values obtained from the filter trap assay are the mean average of three independent experiments. Error bars represent SEM. \*, denotes  $P < 0.05$  compared to negative controls (NT and EGFP). (F) Quantitative analysis of aggregated human SOD1 internalization into NSC-34 cells using flow cytometry. Cells were either incubated with PBS (grey) or aggregated HuWtSOD1 (red line). (G) Visualization of exosomes secreted by NSC-34 cells by negative staining electron microscopy (scale bar = 100nm). (H) Immunogold labeling using 3H1 antibody shows surface localized misfolded SOD1 on exosomes secreted by stably transfected NSC-34 cells (scale bar = 50nm). (I) Quantification of exosomal and proximal free misfolded SOD1 secreted by NSC-34 cells. (J) NSC-34 cells were treated with NSC-34-derived exosomes for 30 min and fixed. Quantitative analysis of SOD1-GFP internalization into NSC-34 cells using flow cytometry. Cells were either incubated with PBS (grey) or HuWtSOD1-GFP exosomes (red line).

### Figure 2. Mutant SOD1-mediated HuWtSOD1 misfolding is transmissible between cells.

(A) Immunoprecipitation (IP) of lysates from naïve HEK cells cultured in the presence of conditioned medium from one, three and five passages of transduction assays initiated by different SOD1 variants. mIgG2a, mouse IgG2a isotype control; rIgG, rabbit mixed IgG control; SOD1, pan-SOD1 antibody; 3H1 and 10C12, misfolded SOD1 specific antibodies. (B) SOD1 knockdown abolishes detectable misfolding. IP of lysates from HEK cells with knocked-down SOD1 expression cultured in the presence of conditioned medium from HEK cells transfected with empty vector control (EV), SOD1-G85R, SOD1-G127X, or HuWtSOD1. (C) IP of lysates from naïve primary neural cell cultures derived from embryonic spinal cord of HuWtSOD1 transgenic or non-transgenic littermate (n-Tg) mice incubated in the presence of conditioned from SOD1-G127X- or empty vector (EV)-transfected HEK293 cells.

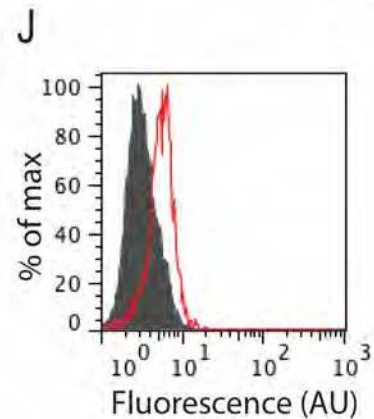
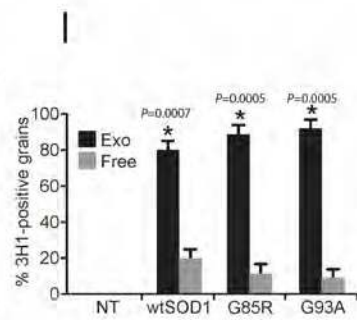
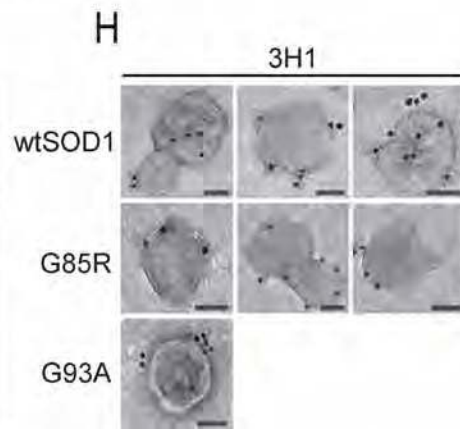
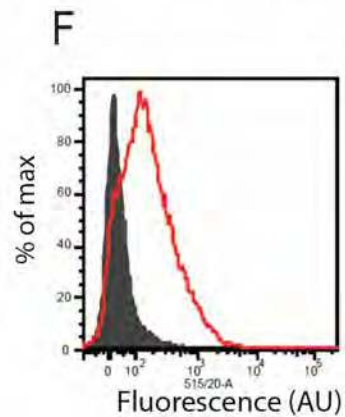
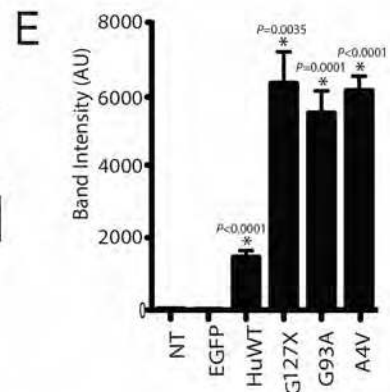
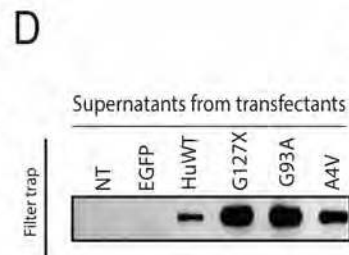
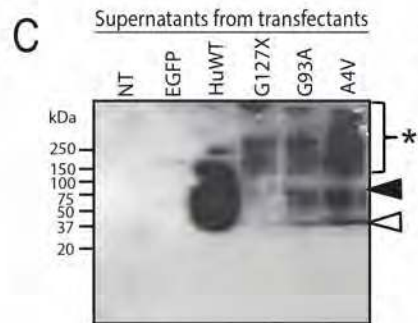
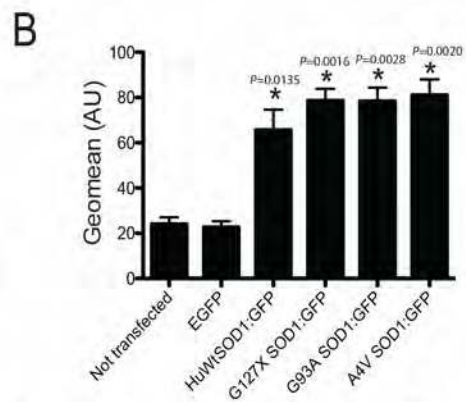
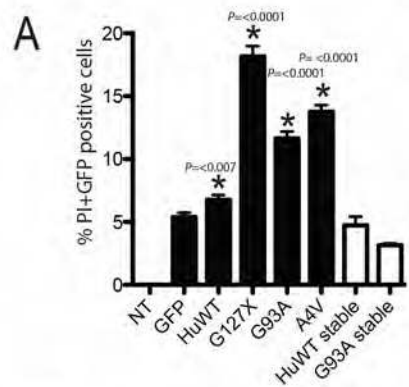
### Figure 3. Misfolded SOD1 is detectable in the culture media of cells transfected with SOD1 constructs.

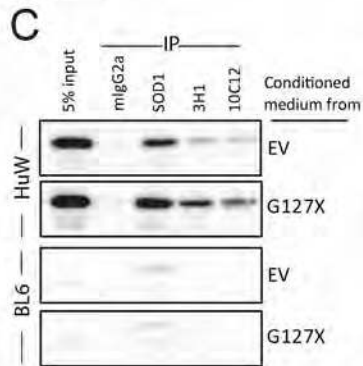
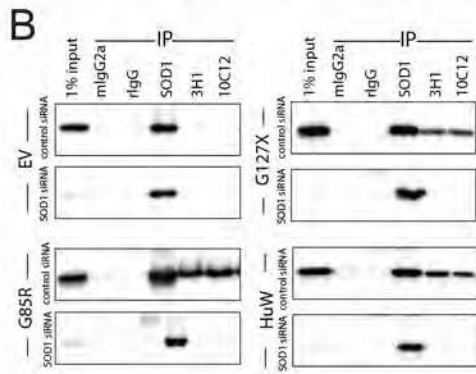
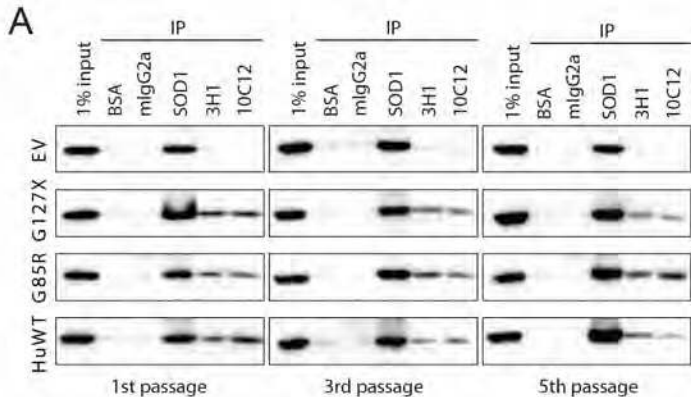
(A) Misfolded SOD1 was detected by IP in both the pellet (P) and supernatant (S) fractions of centrifugated conditioned media, but majority was detected in the P fraction. C-less GX, cysteine-less version of G127X SOD1; mIgG2a, mouse IgG2a isotype control; rIgG, rabbit mixed IgG control; SOD1, pan-SOD1 antibody; 3H1 and 10C12, misfolded SOD1 specific antibodies. This was confirmed by Biacore detection of misfolded SOD1 in the pellet fraction by 3H1 capture (B). Values represent the average of

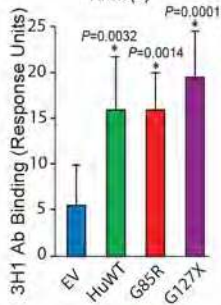
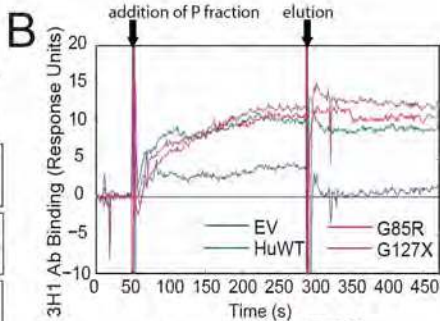
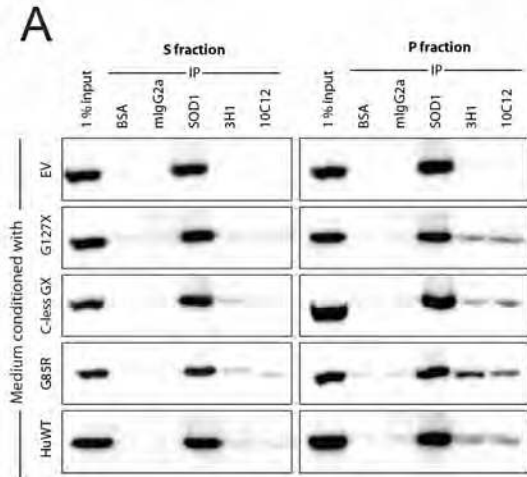
seven independent experiments. \*, indicates significant values. Statistical significance determined by unpaired *t*-test, compared to EV control (significant *P*-values shown); error bars give standard deviation.

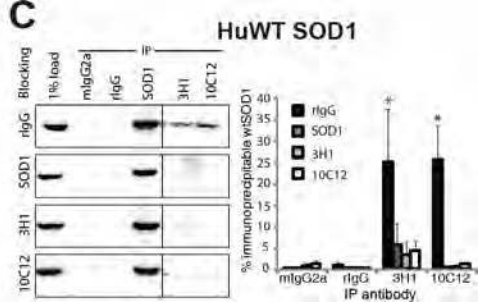
**Figure 4. SOD1 antibodies can block misfolding transmission.** IP of lysates from naive HEK cells cultured in the presence of conditioned medium from G127X-transfected HEK cells (**A**), G85R-transfected HEK cells (**B**), or HuWtSOD1-transfected HEK cells (**C**) immunologically pre-treated with either rabbit mixed IgG (rlgG), pan-SOD1 pAb (SOD1), or DSE mAbs 3H1 or 10C12, all at 20 µg/ml. Corresponding quantitation is shown to the right of each immunoblot. Values represent the mean average of four independent experiments. Error bars represent standard deviation. \*, statistically significant blocking of wtSOD1 misfolding transmission by specific antibodies as determined by ANOVA analysis followed by Tukey (HSD) multiple comparison. For G127X experiment, *P*=0.0048; for G85R experiment, *P*=0.0100; for HuWtSOD1 experiment, *P*=0.032.

**Figure 5. Misfolded SOD1 is detectable in the spinal cords of both FALS and SALS patients.** Immunohistochemistry using antibodies against misfolded SOD1 in cases of FALS with SOD1 mutations (**A-D**) and SALS (**E, F**). In cases with SOD1 mutations, neuronal cytoplasmic inclusions and neurites (arrow) were labeled in the primary motor cortex (**A**) and ventral grey matter of the spinal cord (**B, C**). The spinal grey matter (**d**) also contained numerous swollen axons. Immunopositive axons of normal calibre with a visible myelin sheath were present in the corticospinal tracts (arrows, **E**) and motor nerve roots (arrows, **F**) in sporadic cases. Immunohistochemistry using 10E11C11 (A, B, D-F) and 3H1 (C) antibodies. Scale bar: 20 µm, A and D; 30 µm B and C; 12 µm E and F. (**G**) Immunoprecipitation of 10% (w/v) spinal cord homogenate in PBS using DSE mAbs, normalized to equal concentrations of SOD1. Samples were pre-incubated at 37°C for 30 min in the presence or absence of 200 µg/ml proteinase K (PK). All immunoblots probed with pan-SOD1 polyclonal antibody. C, cervical spinal cord; T, thoracic spinal cord.











## SI Materials and Methods

**Cell culture and transfection.** Cell culturing and transfections for HEK293FT, N2a and NSC-34 cell lines were performed as described (1). For induction experiments, culture medium from transfected HEK293FT cells was collected 48 h post-transfection followed by centrifugation for 5 min at 1000 x g to remove debris. The resulting supernatant was placed onto naive HEK or N2a cells, supplemented with fresh growth medium, and incubated at 37°C for 20 h. This was repeated as required for multi-passage transduction. To assess the relative particle size of the misfolding agent, conditioned media from transfected cells was collected and centrifuged at 100,000 x g for 1 h. The supernatant fraction was concentrated using an Amicon® Ultra-4 Centrifugal Filter Unit (3-kDa; Millipore, Billerica, MA) and eluted into 1 ml of PBS; the pellet fraction was resuspended in 1 ml of PBS. Fractions were added to fresh growth medium and cultured with HEK cells as above. For blocking experiments, conditioned medium was pre-incubated with the designated antibodies at a concentration of 20 µg/ml for 30 min at 37°C, and then placed on naive HEK cells for 20 h. Cells were then collected and lysed for immunoprecipitation as described below.

Mouse NSC-34 cells were cultured in Dulbecco's modified Eagle Medium with 10% FCS, 1% penicillin-streptomycin and 1% glutamine (Invitrogen, Carlsbad, CA). Cells were transiently or stably transfected with mutant or HuWtSOD1-EGFP constructs (2) using Lipofectamine 2000 (Invitrogen, Carlsbad, CA).

Experiments involving animals were conducted according to the Canadian Council on Animal Care guidelines and have been approved by the Animal Care Committee of the University of British Columbia (Approval ID: A10-0212). Pregnant C57 BL/6 female mice (Strain: B6SJL-Tg(SOD1)<sup>2Gur/J</sup>, Stock:002297; Jackson Laboratories, Bar Harbor, ME) were sacrificed according to the guidelines of the Institutional Animal Care and Use Committee (IACUC). Primary cerebral cortical cultures were prepared from 12–14 day fetal mice. All mouse tissue culture reagents were purchased from GIBCO BRL (Grand Island, NY), except where noted. Following embryo genotyping, cervical, thoracic and lumbar- regions of the spinal cord were dissected out in Ca<sup>2+</sup> /Mg<sup>2+</sup> -free Hanks Balanced Salts. Meninges were removed and the tissue was transferred to 0.25% trypsin and digested at 37°C for 15 min. Tissue was then resuspended in DMEM plus 10% fetal bovine serum and triturated 4–6 times through a fire-polished tip. The supernatant was centrifuged at 200 g for 45 sec. Pelleted neural cells were resuspended in Neurobasal media, B27, 2 mM L-glutamine (Sigma; Saint Louis, MO) and seeded at a density of 26105 cells/ well onto poly-D-lysine (Sigma) coated #1.5 coverslips in 24-well plates. Cultures were maintained in serum-free Neurobasal-B27 medium, and one-half of medium was replaced on day 3 or 4 with equal volume of fresh medium. Cells were transfected at 5 DIV using Lipofectamine LTX with Plus reagent (Invitrogen; Carlsbad, CA).

**Confocal microscopy.** Wild-type or mutant SOD1-GFP was expressed in NSC-34 cells after stable transfection (as described (2)) or transient transfection (Lipofectamine 2000 as before). After 72 hours SOD1-GFP fluorescence was imaged using a Leica TCS SP5 II scanning confocal microscope (Leica Microsystems, Wetzlar, Germany) using a 60x objective. An argon laser (488 nm) was used to excite the GFP fusion and emission was collected at 520 +/- 20 nm using a standard PMT. Data was acquired in Leica Application Suite (Leica Microsystems). For visualization of SOD1-GFP uptake via exosomes, NSC-



34 cells ( $5 \times 10^4$  cells/well) in 24-well plates were incubated with exosomes (pooled from  $2 \times 75 \text{ cm}^2$  flasks) in 200  $\mu\text{l}$  serum-free DMEM for 30 min at  $37^\circ\text{C}$ . Cells were fixed with 4% (w/v) PFA in PBS, stained with Hoechst 33342 (1:10,000) and visualised using an Olympus FV 1000 confocal microscope.

**Cell death.** Cells were removed from culture media, resuspended in PBS and propidium iodide was added immediately before analysis by flow cytometry. GFP positive cells (em 515 nm) were gated and were analyzed for positive staining with propidium iodide (PI; em 575 nm). Cells stained with PI were scored as dead and these cells expressed as a proportion of total GFP positive cells. The results are means and standard error of three independent experiments.

**Aggregation of recombinant SOD1.** SOD1 was incubated at 0.5 mg/mL in 10 mM potassium phosphate buffer containing 10 mM DTT and 5 mM EDTA, pH 7.4 at  $37^\circ\text{C}$  whilst shaking. Aggregation was measured as an increase in thioflavin T fluorescence.

**Exosome isolation.** Cell lines were cultured in  $75 \text{ cm}^2$  flasks until confluent. Medium was replaced with fresh 15 ml serum-free medium overnight. Conditioned medium was sequentially centrifuged at 1,000  $g$  for 20 min, 10,000  $g$  for 20 min and 100,000  $g$  for 1 hr. Exosome pellets were washed in PBS by centrifuging at 100,000  $g$  for 1 hr and resuspended in serum-free DMEM. Naive NSC-34 cells suspensions ( $5 \times 10^5$  cells) detached with 1 mM EDTA were treated with exosomes for 30 min at  $37^\circ\text{C}$ , fixed and permeabilized, and internalized SOD1-GFP measured using flow cytometry.

**Cell surface binding and internalization of aggregated SOD1.** NSC-34 cells were initially incubated with 20  $\mu\text{g}/\text{mL}$  of aggregated HuWtSOD1 for 30 min at  $4^\circ\text{C}$ . Cells were fixed with 4% (w/v) PFA in PBS (pH 7.4) before being permeabilized with Triton X-100, and subsequent detection of recombinant SOD1 with sheep polyclonal anti-human SOD1 or using streptavidin-Alexa488 to detect aggregates that have been biotinylated. Cells were quantitatively analyzed by flow cytometry (BD LSR II; BD Biosciences, Franklin Lakes, NJ). Internalization of aggregated HuWtSOD1 was confirmed using confocal microscopy of treated cells while remaining adhered to a coverslip. Internalisation was further measured in the presence or absence of a range of compounds that inhibit various internalization mechanisms. NSC-34 cells were pre-treated with either 25  $\mu\text{g}/\text{mL}$  cytochalasin D, 5  $\mu\text{M}$  of chlorpromazine hydrochloride (CPZ), 100  $\mu\text{M}$  of 5-ethyl-N-isopropyl amiloride (EIPA) or 5 mM methyl- $\beta$ -cyclodextrin (M $\beta$ CD) for 30 min at  $37^\circ\text{C}$ , followed by 20  $\mu\text{g}/\text{mL}$  wildtype aggregated SOD1 for 30 min at  $37^\circ\text{C}$ . Cells were then incubated with 4% (w/v) PFA in PBS (pH 7.4) for 30 min at room temperature followed by incubation with triton x-100 for 15 min. Human SOD1 was detected as before.

**SOD1 expression knock-down.** SOD1 protein levels were knocked-down in HEK cells using a combination of two SOD1-specific siRNA oligonucleotides (Cat. nos. S451, S452; Invitrogen). Transfections were performed using Lipofectamine RNAiMAX (Invitrogen) according to manufacturer's instructions. A random siRNA oligonucleotide mixture (Invitrogen, Cat. no. 4611G) served as a negative control. The transfection complex was incubated for 12 min and added to 60% confluent HEK cells growing in 10 ml complete growth media. Following 80 h incubation, media was replaced with conditioned media from cells transfected with different SOD1 constructs and incubated for an additional 20 h. Cells were then collected and lysed for immunoprecipitation.

**Surface plasmon resonance detection of misfolded SOD1 in transfected cell media.** HEK cells were transfected as described above. 48 h post-transfection, media was harvested and centrifuged at 100,000 g for 1 h. Following centrifugation, supernatant was aspirated to 1ml in each tube into which the pellet was resuspended for analysis. Measurement of misfolded wtSOD1 was performed using a BiaCore 3000 surface plasmon resonance detector (GE Healthcare, Uppsala, Sweden) as previously described (1). A total of seven replicates were performed for each transfectant.

**Immunohistochemistry.** All spinal cord tissues were obtained at autopsy within 48 h of patient death. Immunohistochemistry was performed on cases of familial ALS with known SOD1 mutations (SOD1+ FALS, N = 5), familial ALS with SOD1 mutations excluded (SOD1- FALS, N = 3), sporadic ALS (SALS, N = 20) and normal controls (N = 5). Immunohistochemistry was performed on 3  $\mu$ m sections of formalin-fixed, paraffin-embedded tissue using the Ventana BenchMark® XT automated staining system (Ventana Medical Systems, Inc., Tucson, AZ) and developed with aminoethylcarbazole (AEC). Optimal staining was produced under the following conditions; 10E11C11 (1:500, following microwave pre-treatment), 3H1 (1:50, following standard heat retrieval) and 10C12 (1:10, following standard heat retrieval).

**SOD1 solubility.** Solubilized spinal cord homogenates were centrifuged for 8 min at 100,000 x g in a TLA100.3 rotor to separate the soluble supernatant (S) from the crude pellet. Crude pellet was resolubilized and centrifuged to obtain the non-ionic detergent-insoluble pellet (P). 1 M iodoacetamide was added to the S and P fractions to a final concentration of 100 mM. 2X SDS sample buffer without  $\beta$ -mercaptoethanol (non-reducing sample buffer) was added to 1X final concentration and separated on Novex 4-20% acrylamide gels (Invitrogen), followed by immunoblotting .

## References

1. Grad LI, *et al.* (2011) Intermolecular transmission of superoxide dismutase 1 misfolding in living cells. *Proc Natl Acad Sci U S A* 108(39):16398-16403.
2. Turner BJ, *et al.* (2005) Impaired extracellular secretion of mutant superoxide dismutase 1 associates with neurotoxicity in familial amyotrophic lateral sclerosis. *J Neurosci* 25(1):108-117.

## Supplementary Figures

### Figure S1. SOD1 inclusions form in transiently transfected cells but not stably transfected cells.

Confocal microscopy of SOD1-EGFP stably transfected or transiently transfected NSC-34 cells. Green = SOD1; scale bar = 50  $\mu$ m. White arrows indicate intracellular SOD1 inclusions in transiently-transfected cells.

**Figure S2. Aggregated recombinant human SOD1 can seed WT SOD1 aggregation.** (A) Aggregation of purified recombinant HuWt and G93A SOD1 is followed in real time using Thioflavin T fluorescence. Under the conditions tested (0.5 mg/mL SOD1 in 10 mM DTT and 5 mM EDTA), HuWtSOD1 does not aggregate. (B) Pre-aggregated mutant SOD1 was added to starting solution of HuWtSOD1, to give 10% of total SOD1, to induce aggregation. Only in the presence of seeds does substantial HuWtSOD1 aggregation occur. (C) HuWtSOD1 aggregates taken from (b) were added to starting solutions of HuWtSOD1 and used to seed further aggregation. (D) Representative TEM image of fibrillar aggregates formed by HuWtSOD1. Scale bar represents 500 nm. (E) Aggregated SOD1 is internalized by NSC-34 cells. Biotinylated recombinant human SOD1 pre-aggregated *in vitro* was exogenously applied to NSC-34 cells, incubated, and then fixed and probed using streptavidin-Alexa488. Confocal microscopy was used to examine immunofluorescence associated with human SOD1 aggregates. Scale bar = 7.5  $\mu$ m. (F) Aggregated SOD1 is internalized via macropinocytosis. Internalization of aggregated HuWtSOD1 was measured by flow cytometry, in the presence or absence of a pre-incubation step with cytochalasin D, chlorpromazine hydrochloride (CPZ), 5-ethyl-N-isopropyl amiloride (EIPA) or methyl- $\beta$ -cyclodextrin (M $\beta$ CD). Error bars represent SEM from 6 replicates, and \* denotes statistical significance determined by unpaired *t*-test, compared to no inhibitor control (significant *P*-values shown). Although the actin dependent pathway inhibitor cytochalasin D decreased the SOD1 internalized into the NSC-34 cells, this was not statistically significant. (G) SOD1 is specifically taken up by neuron-like cells. NSC-34 cells were incubated with soluble HuWt or G93A SOD1 or aggregated recombinant SOD1 protein (Agg) for 30 min. Cells were then fixed/permeabilized and probed for human SOD1. As a control, cells were incubated under the same conditions with glutathione-s-transferase (GST) and probed for GST. Error bars represent geometric means of three independent experiments.

**Figure S3. Characterization of exosomes and exosomal surface misfolded SOD1.** (A) Immunoblot analysis of exosomal markers in cell and exosome (exo) fractions from NSC-34 cells. (B) Immunogold labeling of surface localized PrP on exosomes from NSC-34 cells by electron microscopy. Immunogold labeling using 10C12 (C), but not C4F6 (D), shows surface-localized misfolded SOD1 on exosomes secreted by NSC-34 cells stably transfected with mutant or HuWtSOD1-GFP. (E) Immunogold labeling using 3H1 antibody shows presence of misfolded SOD1 on the outside of exosomes secreted by NSC-34 cells transiently transfected with untagged HuWtSOD1 or mutant (G93A). Scale bar (B-E) = 50 nm. (F) Exosomal SOD1 is internalized by NSC-34 cells. Naive NSC-34 cells were treated with exosomes derived from SOD1-GFP stably transfected NSC-34 cells for 30 min, fixed and visualized by confocal microscopy. Scale bar = 20  $\mu$ m.

**Figure S4. Controls establishing specificity of propagated SOD1 misfolding reaction.** (A) Template directed misfolding transduction and blocking (see Figure 4) experimental design. (B) Quantitation

summary of Fig. 1d with values represented as the mean average of four independent experiments. Error bars represent standard error. \*, statistically significant induction ( $P = 0.003$ ) of HuWtSOD1 misfolding between species and between control vs. G127X conditioned media induction as determined by ANOVA analysis followed by Tukey (HSD) multiple comparison. (C) Exposure to a non-SOD1  $\beta$ -barrel protein (GFP) does not induce HuWtSOD1 misfolding. Immunoprecipitation of lysates from naïve HEK cells cultured in the presence of conditioned media from GFP-transfected HEK cells. HuWtSOD1 immunoprecipitation with DSE mAbs 3H1 and 10C12 is negligible. Quantitation summary is included; error bars represent standard error. (D) SOD1 misfolding is not due to residual mutant SOD1 transfection plasmid in conditioned media. Immunoprecipitation of lysates from naïve HEK cells cultured in the presence of conditioned media from G127X-transfected HEK cells, pre-incubated in the presence or absence (PBS only) of 1 unit DNase I/ $\mu\text{g}$  of transfected DNA. Quantitation summary is included; error bars represent standard error. (E) The percentage of total immunoprecipitable SOD1 as a function of the number of misfolded SOD1-induced transduction assay passages from conditioned media derived from four different SOD1 construct transfections. Values are the average of at least three independent experiments. Error bars represent standard deviation. mIgG2a, mouse IgG2a isotype control; rIgG, rabbit mixed IgG control; SOD1, pan-SOD1 antibody; GX-CT, antibody against non-native C-terminal end of SOD1-G127X; 3H1 and 10C12, misfolded SOD1 specific antibodies.

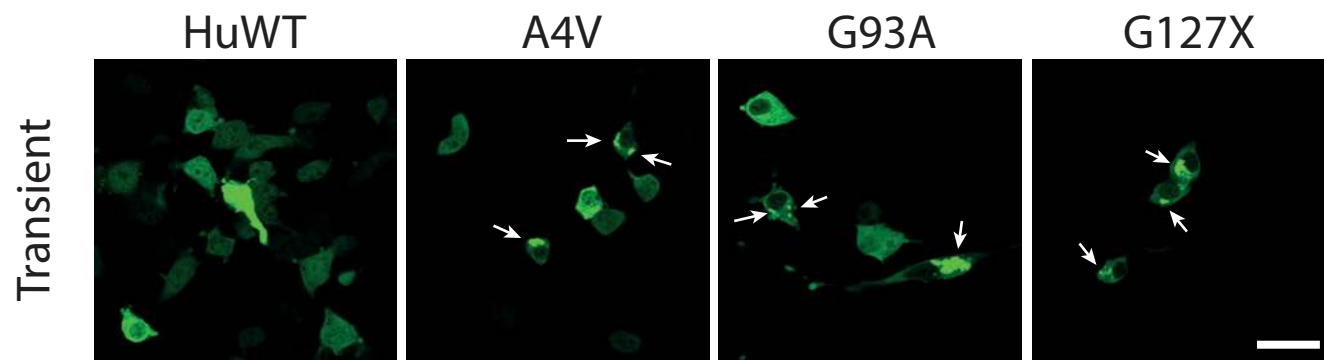
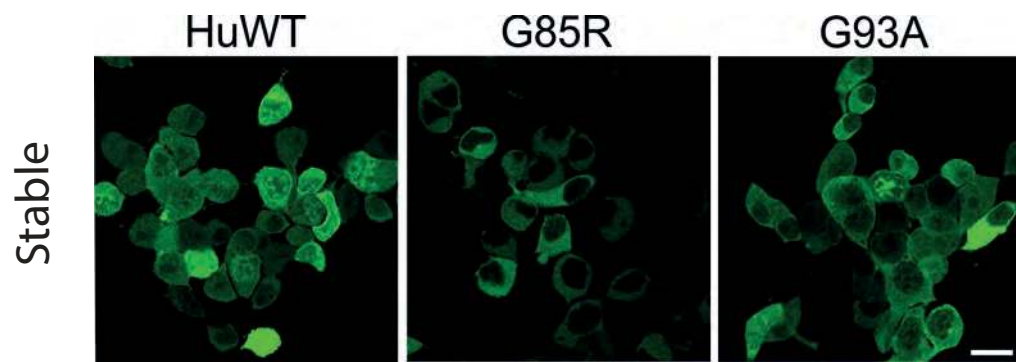
**Figure S5. Quantitation of immunoprecipitation experiments.** (A) Quantitation of immunoprecipitations derived from siRNA knockdown experiment described in Figure 2B. Error bars represent standard error. Values represent the average of four independent experiments. Error bars represent standard error. \*, indicates significant values. Statistical significance determined by unpaired  $t$ -test, compared to controls (significant  $P$ -values shown). mIgG2a, mouse IgG2a isotype control; rIgG, rabbit mixed IgG control; SOD1, pan-SOD1 antibody; 3H1 and 10C12, misfolded SOD1 specific antibodies. (B) Quantitation of immunoprecipitations derived from SOD1 transduction experiments in mouse neural cultures described in Figure 2C. Any signal detected from mIgG2a isotype control was deemed background and subtracted from signal from SOD1-DSE antibody pull-down of misfolded SOD1. Values represent the average of three independent experiments. Error bars represent standard error. Statistical significance determined by unpaired  $t$ -test, compared to empty vector (EV) conditioned medium controls (significant  $P$ -values shown).

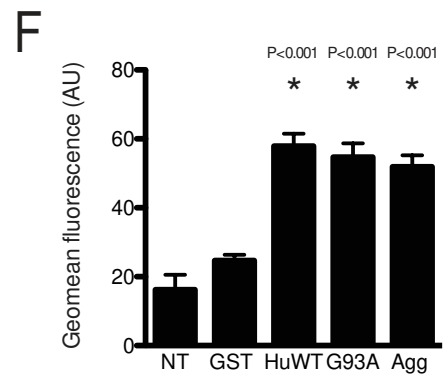
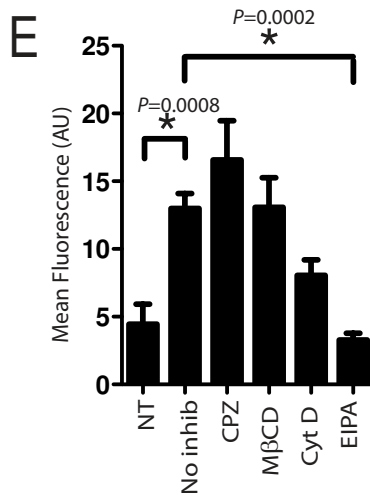
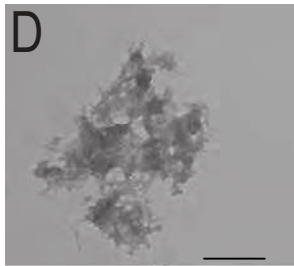
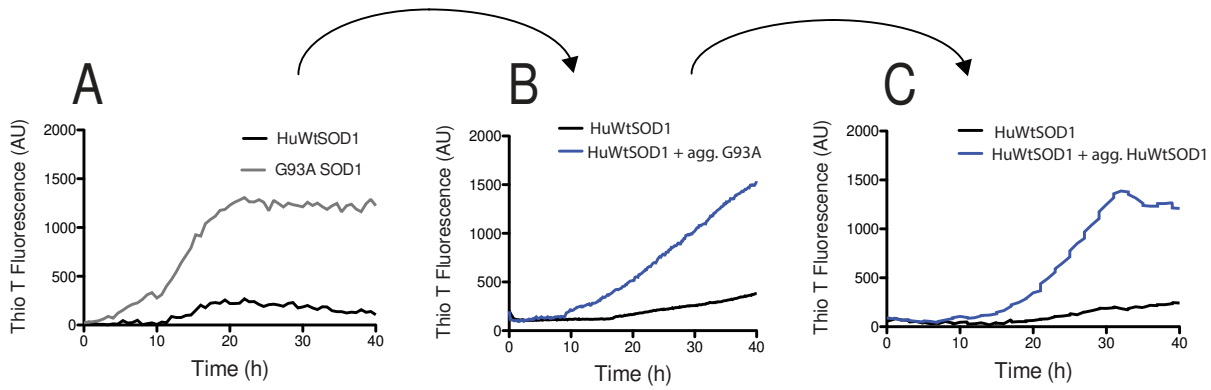
**Figure S6. Transmission of misfolded SOD1 occurs via large molecular mass particles that are exposed to DSE antibodies.** (A) Quantitation of misfolded wtSOD1 immunoprecipitation from fractionated post-transfection conditioned media. Values represent the mean average from four independent experiments. Error bars give standard error. \* indicates significant values; statistical significance was determined by using the Mann-Whitney test to compare pairs of soluble (S) and pellet (P) fractions of conditioned media from cell transfections of different SOD1 constructs (significant  $P$ -values shown). (B) Immunoprecipitation of concentrated culture media from G127X-transfected HEK cells. HuWtSOD1 and G127X SOD1 are in physical association with one another, a precursor to intermolecular conversion of misfolding in conditioned media. GX-CT pAb captures minimal G127X, but also co-immunoprecipitates full-length wtSOD1. Since G127X in which all cysteine residues have been substituted with serines was as efficient as native G127X, the formation of interchain disulfide bonds was not essential to initiate the

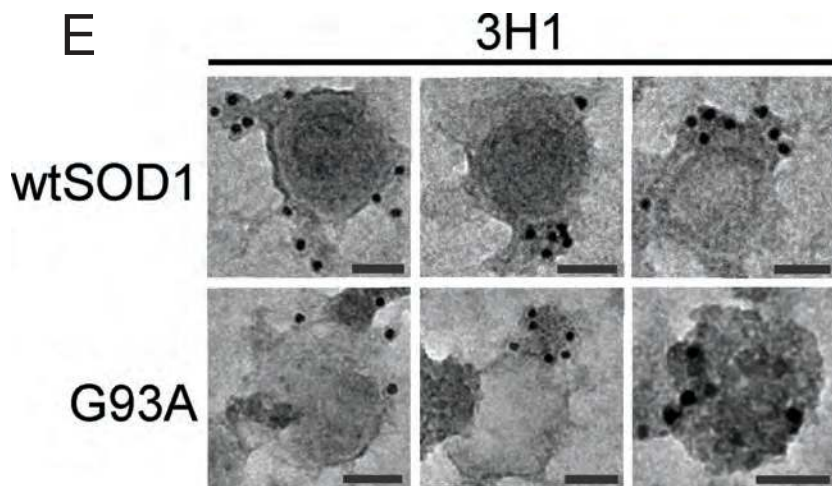
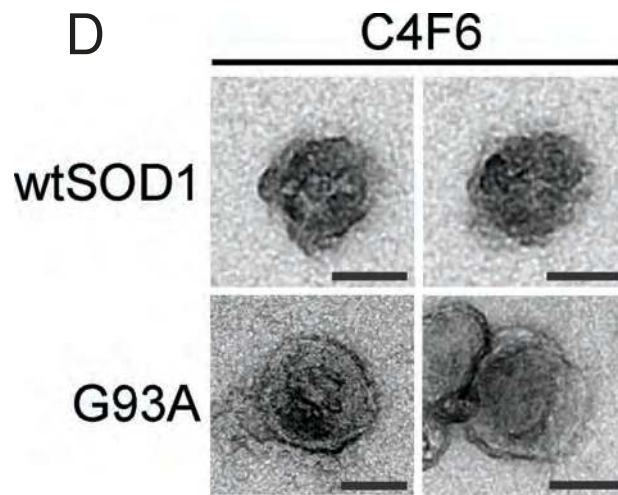
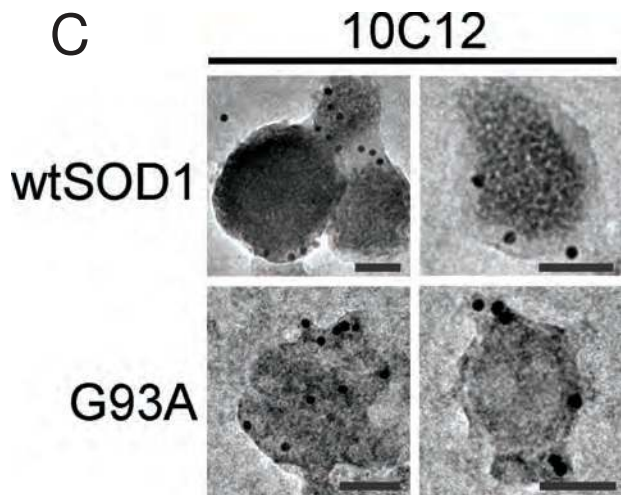
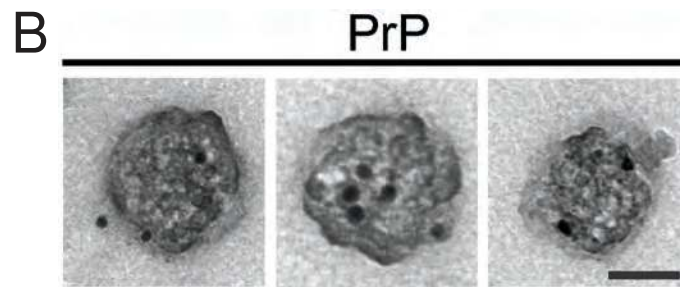
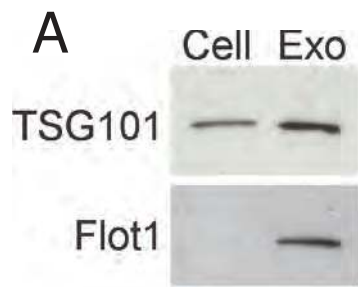
propagation of HuWtSOD1 misfolding. \*, indicates unknown SOD1 degradation product specific to conditioned media.

**Figure S7. Misfolded oligomeric SOD1 is detectable in the spinal cords of both FALS and SALS patients.**

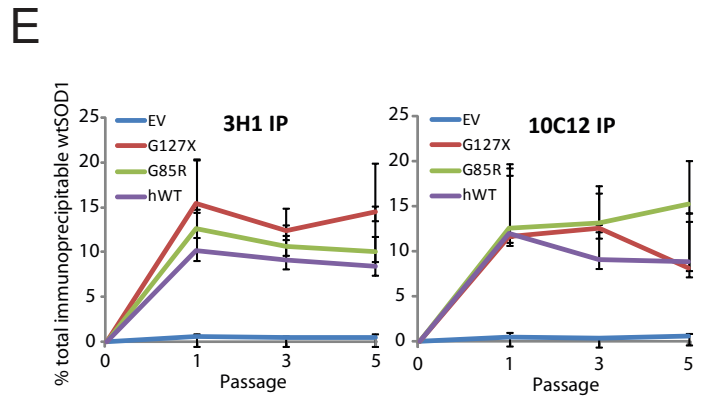
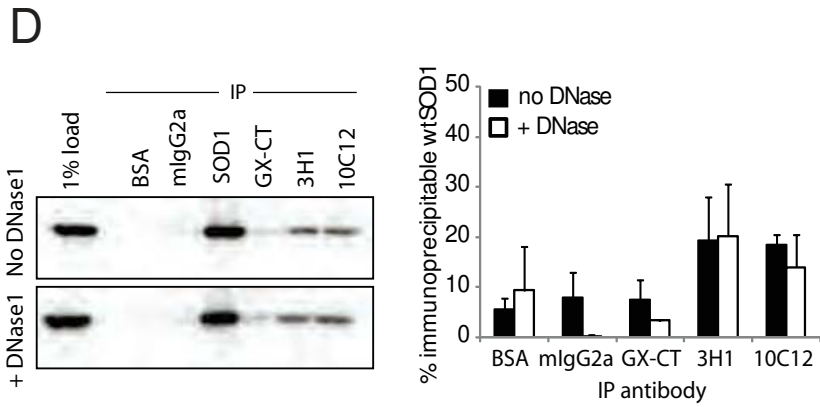
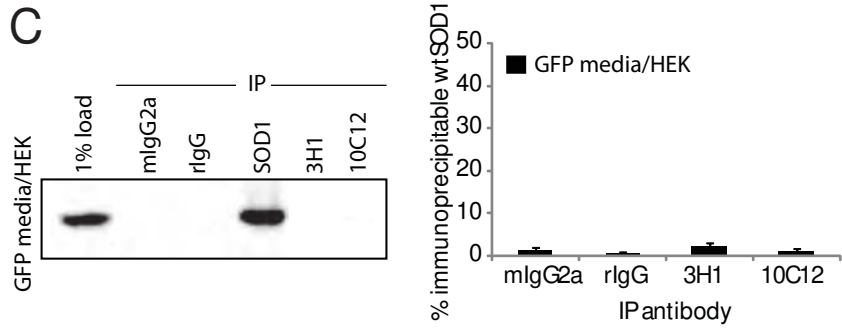
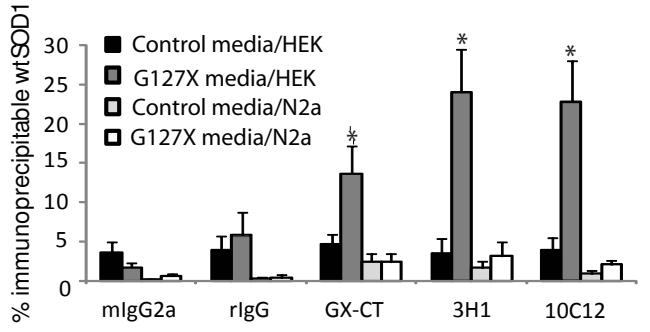
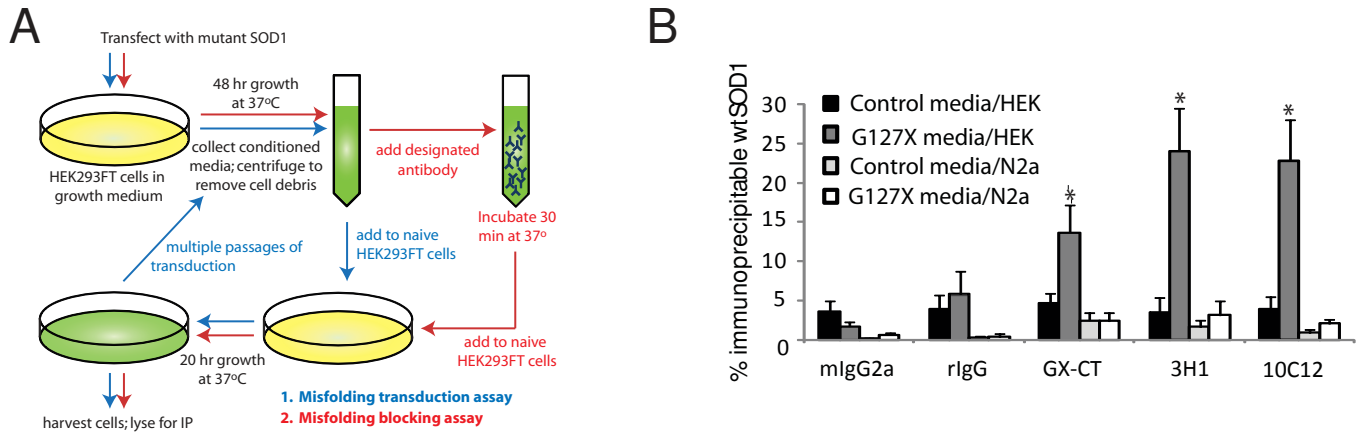
**(A)** Quantitation of pull-down of DSE mAb immunoprecipitable SOD1 expressed as a percentage of total immunoprecipitable SOD1 pulled down by the pan-SOD1 antibody. Data is the average of 4 independent experiments for each patient sample; results for each patient group were pooled. Error bars represent standard deviation. Statistical significance was determined using Mann-Whitney test to compare pairs of PK-treated vs. untreated samples (significant *P*-values shown). **(B)** 2 µg of 10% spinal cord homogenate diluted in IP buffer from normal patients treated with increasing concentrations of PK. SOD1 from normal spinal cord is resistant to PK, even at a concentration 100-fold higher than used in experiments shown in (A). **(C)** Spinal cord homogenates, in the presence of 1% NP-40, were separated to generate a soluble fraction (S) and a detergent-insoluble pellet (P). The S and P fractions, denatured in sample buffer without a reducing agent, were separated on 4-20% acrylamide gels by standard SDS-PAGE. C, cervical spinal cord; T, thoracic spinal cord. **(D)** Quantitation of the detergent-insoluble oligomers (P fraction; vertical bar in (a) represents the region quantified). Data is the average of 4 independent experiments for each patient sample; results are pooled into disease categories. Error bars represent standard deviation. Statistical significance determined by unpaired *t*-test, compared to normal controls (significant *P*-values shown).

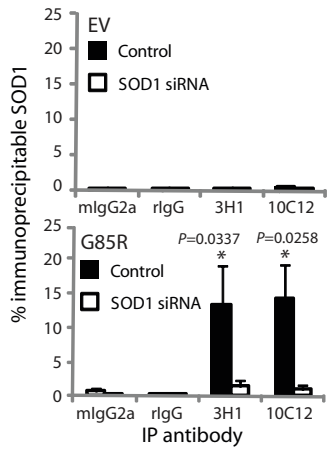
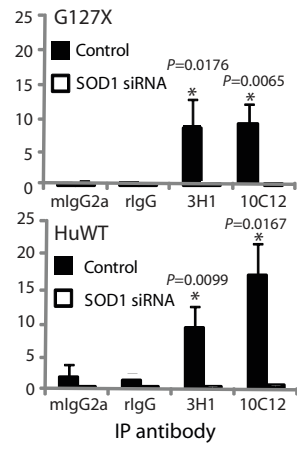




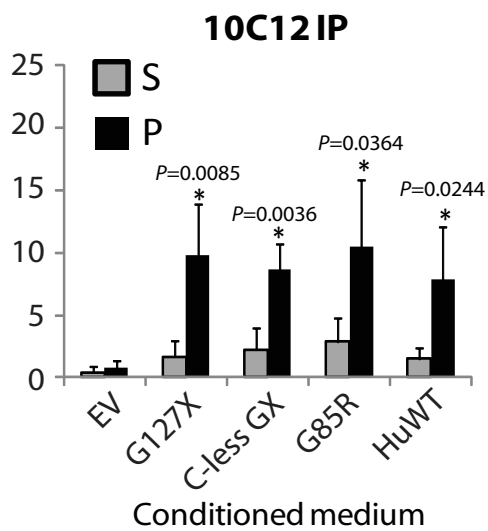
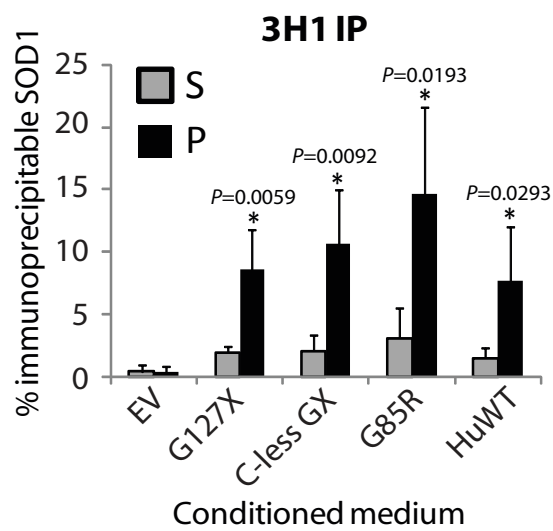




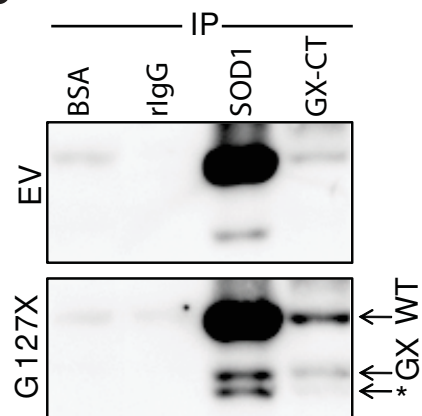


**A****B**

**A**



**B**



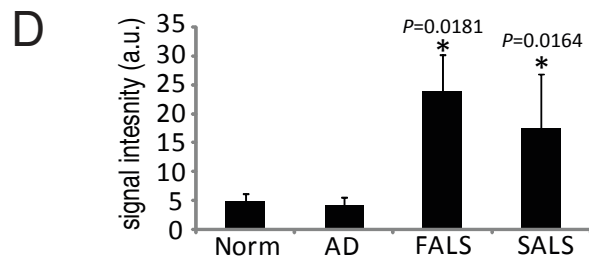
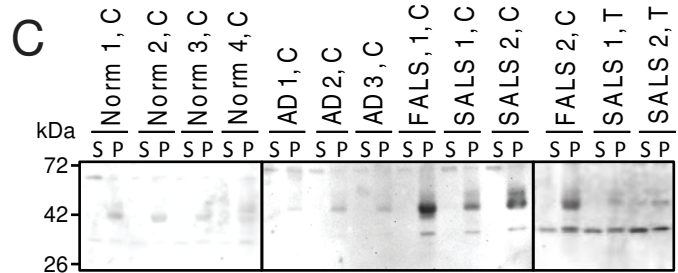
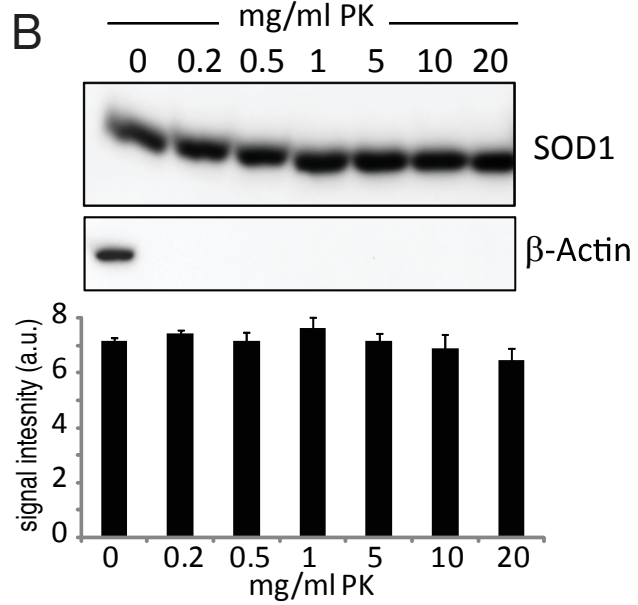
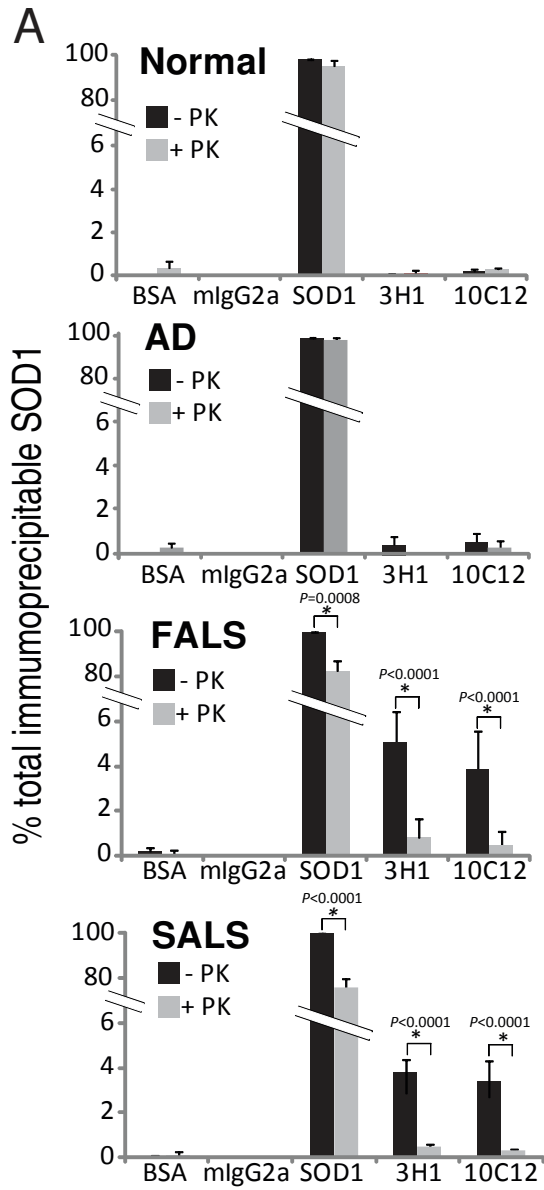


**Table S1****Clinical and demographical information on spinal cord tissues used for immunohistochemistry**

Disease Status	Mutation (Gene)	Spinal Cord Region	Sex	Age	Onset age
Normal	-	C, L	M	35	-
Normal	-	C, L	M	53	-
Normal	-	C, L	M	56	-
Normal	-	C, L	M	63	-
Normal	-	C, L	F	90	-
SOD1+FALS	A4V (SOD1)	C, L	M	46	43
SOD1+FALS	A4V (SOD1)	C, L	M	52	50
SOD1+FALS	D90A (SOD1)	C, L	M	60	n/a
SOD1+FALS	D90A (SOD1)	C, L	M	63	46
SOD1+FALS	G72C (SOD1)	C, L	F	75	70
SOD1-FALS	C9ORF72	C, L	M	47	46
SOD1-FALS	C9ORF72	C, L	M	56	55
SOD1-FALS	R521C (FUS)	C, L	F	64	63
SOD1-SALS	unknown	C, L	M	53	53
SOD1-SALS	unknown	C, L	M	57	57
SOD1-SALS	unknown	C, L	M	64	63
SOD1-SALS	unknown	C, L	M	66	63
SOD1-SALS	unknown	C, L	M	73	71
SOD1-SALS	unknown	C, L	M	77	76
SOD1-SALS	unknown	C, L	M	79	78
SOD1-SALS	unknown	C, L	F	43	n/a
SOD1-SALS	C9ORF72	C, L	F	59	57
SOD1-SALS	unknown	C, L	F	65	64
SOD1-SALS	unknown	C, L	F	65	64
SOD1-SALS	unknown	C, L	F	66	65
SOD1-SALS	unknown	C, L	F	66	66
SOD1-SALS	unknown	C, L	F	66	65
SOD1-SALS	unknown	C, L	F	66	63
SOD1-SALS	unknown	C, L	F	72	72
SOD1-SALS	unknown	C, L	F	73	72
SOD1-SALS	unknown	C, L	F	74	73
SOD1-SALS	unknown	C, L	F	82	73
SOD1-SALS	unknown	C, L	F	83	80

All tissues collected at autopsy with 48 hours of patient death and used directly for IHC analysis. C, cervical; L, lumbar.

**Table S2****Relative abundance of antibody staining in various regions and structures of patient spinal cord sections****10C12 (DSE1a mAb) staining**

<b>Structure/Region</b>	<b>SOD1 FALS</b>	<b>non-SOD FALS</b>	<b>non-SOD1 SALS</b>	<b>Control</b>
Neuronal cytoplasmic inclusion	++	-	-	-
Axonal swellings	+	-	-	-
Axons	++	+	+	-
Corticospinal tract	+	+	+	-
Other tracts	+	-	-	-
Motor Roots	+	+	+	-

**3H1 (DSE2 mAb) staining**

<b>Structure/Region</b>	<b>SOD1 FALS</b>	<b>non-SOD FALS</b>	<b>non-SOD1 SALS</b>	<b>Control</b>
Neuronal cytoplasmic inclusion	++	-	-	-
Axonal swellings	++	-	-	-
Axons	++	+	+	-
Corticospinal tract	+	+	+	-
Other tracts	+	-	-	-
Motor Roots	+	+	+	-

**10E11C11 (DSE2 mAb) staining**

<b>Structure/Region</b>	<b>SOD1 FALS</b>	<b>non-SOD FALS</b>	<b>non-SOD1 SALS</b>	<b>Control</b>
Neuronal cytoplasmic inclusion	++	-	-	-
Axonal swellings	++	-	-	-
Axons	+++	++	+	-
Corticospinal tract	+++	++	++	-
Other tracts	+	+	+	-
Motor Roots	++	+	+	-

Grey box indicates sub-structures within the ventral grey matter. Positive staining in corticospinal tract, other tracts and motor roots was in axons. -, no staining; +, some staining; ++, moderate staining; +++, abundant staining.

**Table S3****Clinical and demographical data on frozen spinal cord sections**

Sample ID	Disease status	Spinal Cord Region	Sex	Age	PMI
Normal 1	Normal	Cervical	M	65	n/a
Normal 2	Normal	Cervical	M	38	n/a
Normal 3	Normal	Cervical	M	55	n/a
Normal 4	Normal	Cervical	F	76	4 days
AD 1	Alzheimer's Disease	Cervical	M	71	4 days
AD 2	Alzheimer's Disease	Cervical	M	68	4 days
AD 3	Alzheimer's Disease	Cervical	F	66	3 days
FALS (A4V)	SOD1 FALS (A4V)	Cervical	M	52	2 days
FALS (G72C)	SOD1 FALS (G72C)	Cervical	F	75	2 days
SALS C-SC 1	non-SOD1 SALS	Cervical	M	66	2 days
SALS C-SC 2	C9ORF72 SALS	Cervical	F	59	1 day
SALS T-SC 1	non-SOD1 SALS	Thoracic	M	73	n/a
SALS T-SC 2	nonSOD1 SALS	Thoracic	F	39	n/a

PMI, post-mortem interval.